A NOVEL AND ENHANCED CALIBRATION OF THE TILTING WEIR AS A FLOW MEASUREMENT STRUCTURE

Joseph E Pugh, S Karan Venayagamoorthy, Timothy K Gates, Céline Berni, Marie Rastello

A NOVEL AND ENHANCED CALIBRATION OF THE TILTING WEIR AS A FLOW MEASUREMENT STRUCTURE

Joseph E. Pugh[1,2], S. Karan Venayagamoorthy[1,2], Timothy K. Gates[2], Céline Berni[3], and Marie Rastello[4,2]

[1]Environmental Fluid Mechanics Laboratory at Colorado State University. Email: jepugh@colostate.edu

[2]Dept. of Civil and Environmental Engineering, Colorado State University, 1372 Campus Delivery, Fort Collins, CO, 80523, USA.

[3]INRAE, Unit Recherche RiverLy, HHLab, 69100 Villeurbanne, France.

[4]Univ. Grenoble Alpes, CNRS, Grenoble INP, LEGI, 38000 Grenoble, France.

ABSTRACT

A large collection of laboratory measurements of piezometric head (h) and discharge (Q) are made over hydraulic models of a tilting weir at nine different angles, ranging from 25.7° to 90° within a 0.3-m wide flume. These measurements are corroborated with additional laboratory data taken within a 1-m wide flume across four inclination angles. The range of both inclination angle (θ) and flow scale examined in this study elucidate the nature of the head-discharge rating equation beyond previous work. Results show that as θ decreases under a constant Q, the h over the weir decreases in a monotonic fashion due to the shallower angle of attack of the flow, which results in less curvature of the streamlines over the crest and therefore less deviation from the upstream hydrostatic pressure condition. To incorporate this effect into the head-discharge rating equation, a transformation of the h term is applied by multiplying the measured h that occurs over an inclined weir by a correction factor to match the effective h that would occur if the weir were aligned perpendicular to the flow at the same discharge. Thus, a modified form of the classical sharp-crested weir rating equation can

be used as a means for determining the value of Q for inclined cases to a high degree of accuracy. The degree of accuracy is dependent upon dimensionless Reynolds and Weber numbers describing the flow inertia in the approach to the weir in relation to respective viscous and surface tension scale effects. This approach portends marked flow measurement enhancement for flow conditions above a suggested inertial threshold.

INTRODUCTION

Tilting weirs (i.e. overshot gates) have been in use since the late twentieth century for the purpose of regulating upstream water levels in open channel flow, typically within the context of irrigation systems or spillway operation (Wahlin and Replogle 1994; Stringam and Gill 2012). The same type of structures are also widely used in Asia (Bijankhan and Ferro 2017; Lee et al. 2014), where they are primarily referred to as pivot weirs. These simple overflow structures operate as a flat rectangular plate that is hinged to the bottom of the channel and inclined from the horizontal through the use of pneumatic pressure vessels, a pulley mechanism, or a piston mechanism. It is generally assumed that the crest of these structures is thin, so that a springing jet (i.e. nappe) forms on the downstream side of the structure. In irrigation systems, tilting weirs allow for regulation of the stage upstream of the structure to provide the pressure head necessary to divert flow from a main supply canal into lateral canals. In spillway operation, these structures can be installed in parallel to allow for careful release of flows and regulation of the reservoir stage in response to varying supply and demand levels.

Tilting weirs require careful consideration of aeration demands for the underside of the plunging nappe to be supported by atmospheric pressure (Bos 1976). If these structures are properly designed, the downstream channel bed elevation will be set low enough to allow for the energy of the supercritical plunging nappe to be dissipated, while also ensuring that a sufficient supply of fresh air is provided to the pocket of atmospheric pressure supporting the nappe. For these reasons, tilting weirs offer the potential of being practical hydraulic structures that serve the dual functions of stage regulation and discharge measurement. The initial development of these structures as stage regulation devices has been well documented and widely implemented (Clemmens et al. 2001;

Floodlist News 2017). However, their use as flow measurement devices remains in need of further investigation.

Fundamentals of the Weir Rating Equation

The development of a method for predicting the volumetric discharge over tilting weirs begins with an understanding of Torricelli's principle of a jet at the base of a reservoir issuing from a small orifice. Here, the velocity (u) of the jet can be related to the potential energy in the static supply reservoir by the function $u = \sqrt{2gh}$, with h being the elevation of the water surface above the jet outlet. This principle assumes the flow is inviscid and irrotational, and that the pressure distribution over the crest is hydrostatic. In his 1717 publication "de moto aquae mixto", Giovanni Poleni applied Torricelli's principle to approximate the discharge of a fluid over a perpendicular weir as occurring in a series of horizontal elements, the velocity of each being proportional to the distance of the fluid element from the free surface (Rouse and Ince 1963). From the resultant parabolic velocity profile, the depth-integrated unit discharge (q) can be approximated using what is known as Poleni's equation.

$$\int_0^h u \, \mathrm{d}h \approx \frac{2}{3}\sqrt{2g}h^{3/2} \approx q \tag{1}$$

However, it is known that because of the simplifying assumptions implicit in the Poleni equation, a dimensionless correction factor must be applied to the idealized efflux to account for the contraction of jet at the crest of the orifice. This has typically been called the discharge coefficient (C_d) when referring to weir flow, but it is in effect a coefficient of contraction (Kindsvater and Carter 1957). Its application to Eq. (1), with the addition of the crest length (b) to account for the transversal dimension, then yields the standard volumetric discharge rating equation for a sharp-crested weir.

$$Q = C_d \frac{2}{3}\sqrt{2g}bh^{3/2} \tag{2}$$

This relatively simple equation forms the theoretical basis for the discharge equation of different types of sharp-crested weirs with variable geometries (Martínez et al. 2005). However, the

simplifying assumptions of this approach should not be overlooked. As previously mentioned, this derivation approximates the flow between the upstream head measurement location and the crest as being inviscid, irrotational, and hydrostatic. For the case of accelerating flow over a weir, it is often taken to be a safe assumption that over the short reach from the measurement section to the crest, the energy loss due to internal rotational shear is negligible (Kindsvater and Carter 1957).

The assumptions of inviscid flow and a hydrostatic pressure distribution can be best examined by considering the theoretical case of a sharp-crested weir of infinite height. Here the assumption of potential flow is valid because the effect of the boundary is negligible. However, for this case the streamlines will approach the crest radially, so that a significant vertical velocity component will be present in the flow, causing the pressure distribution to decrease significantly from the hydrostatic condition. This pressure drop correspondingly results in an acceleration of the flow over the crest and a reduction in the depth of flow at the crest to satisfy the continuity principle (Rouse 1932). The contraction coefficient of the water surface profile over the crest of an infinitely high weir has been shown from potential flow theory to be equal to Kirchhoff's coefficient for a jet issuing from a sharp-edged orifice, where $C_d = \frac{\pi}{\pi+2} = 0.611$ (Rouse 1946b).

If a low weir is considered, so that the effect of the boundary cannot be neglected and the assumption of inviscid flow no longer holds, it can be observed that the flow separates near the base of the weir and a standing eddy forms. This phenomenon was briefly verified in this study by preliminary particle-image velocimetry analysis, as shown by Fig 1. The effect of this flow separation on the streamlines upstream of the weir was described by Rouse (1932) as being akin to tilting the weir downstream, due to the fact that the separation zone causes the streamlines above the separation zone to retain more horizontal momentum. This results in less curvature of the streamlines at the crest and less contraction of the overflowing jet, so that the pressure at the vena contracta more closely approximate the hydrostatic condition. The result is that for a low weir, more discharge can be passed given the same upstream energy condition compared to that for an infinitely high weir (Rouse 1932).

Dimensional Analysis

If the assumption is made that the tilting weir can be treated as a modified case of the classical sharp-crested weir, the general form of Eq. (2) can be applied to establish a head-discharge rating equation for the tilting weir by adding a term that accounts for the inclination angle (θ) of the weir with respect to the horizontal. In order to understand the relevant flow parameters and fluid properties that influence this equation, a dimensional analysis of the tilting weir is now considered.

Simplifying assumptions are made that the weir crest length (b) is equal to the width of the approach channel (B), and the velocity field is uniform in the transversal direction. The flow geometry can then be described by the parameters shown in Fig. 2. Here, L is the vertical height of one weir when positioned perpendicular to the channel bed; p is the elevation of the weir crest above the channel bed at a given θ; and h is the piezometric head measured with reference to the crest elevation in the uniform flow section upstream from the weir. The total hydraulic head (H), is the sum of the piezometric head (h) and the kinetic energy head ($\alpha\overline{U}^2/2g$), where $\overline{U}$ is the velocity averaged over the channel cross section in the approach. The dimensionless term, $\sin\theta = p/L$ describes the effect that the changing angle of attack of the flow on the weir has on streamlines over the crest, and relates p and L. The relevant fluid properties in determining the flow over the weir are the density, ρ, the dynamic viscosity, μ, and surface tension, σ. Since this is a case of open channel flow, gravitational effects are critical and thus the acceleration due to gravity (g) is included as a relevant physical parameter. A functional description of the unit discharge over a fully-suppressed ($b/B = 1$) tilting weir can be written as:

$$q = f(p, h, \sin\theta, g, \rho, \mu, \sigma) \tag{3}$$

Utilizing Buckingham π analysis and a yet to be determined function (ϕ), the following dimensionless equation can be written using the scaling terms $h \equiv \mathrm{L}$, $h/\sqrt{gh} \equiv \mathrm{T}$, and $\rho h^3 \equiv \mathrm{M}$:

$$C_d = \frac{3}{2\sqrt{2}}\, Fr = \phi(h/p, \sin\theta, Re, We) \tag{4}$$

wherein:

$$Fr = \frac{q}{\sqrt{g}h^{3/2}} \tag{5}$$

$$Re = \frac{\sqrt{g}h^{3/2}}{\nu} \quad \text{where} \quad \nu = \mu/\rho \tag{6}$$

$$We = \frac{\rho g h^2}{\sigma} \tag{7}$$

The first term in Eq. (4) is the classical discharge coefficient as shown in Eq. (2), which can be considered as a dimensionless Froude number (Fr) for the flow over the weir crest ($q/\sqrt{g}h^{3/2}$), that has then been transformed by the coefficient $3/2\sqrt{2}$ to make the inertial term in the numerator reflect the depth-averaged velocity from Poleni's approach in Eq. (1).

Regimes of flow over a weir can be divided into four types: clinging, laminar, free, and inundated flow (Johnson 1996; Sinclair et al. 2022). When the flow over the weir is clinging, its inertia is not sufficient to overcome scale effects due to surface tension. Here, the free surface clings to the weir plate and the nappe downstream of the crest is not fully formed. This causes the same discharge to pass over the weir at a lower head compared to when the nappe is fully formed, thus artificially increasing the discharge coefficient (Sarginson 1972). An additional flow regime can occur at low heads, even when the nappe is fully formed. Here, viscous effects rather than surface tension effects are dominant. The flow inertia is not sufficient to overcome viscous effects in the same manner that is observed within the free flow regime; hence the velocity profile deviates from that expected for turbulent open-channel flow (Rouse 1946a). This reduction in the upstream bulk velocity causes h over the weir to artificially increase in order to satisfy conservation of mass, thus decreasing C_d below what is expected for the free flow relationship. Inundated flow occurs on the opposite end of the inertial spectrum, but the effect on C_d is nominally the same as for clinging flow. Here, the pressure head above the weir becomes too great for the air pocket beneath the nappe to be sustained, the nappe collapses, and the head over the weir decreases. Free flow then occurs in between the limits of clinging/laminar and inundated flow, when the weir is operating within the conditions assumed in Eq. (2). This means that dynamic similarity is present so that

the flow dynamics are independent of viscous and surface tension scale effects, and that the nappe downstream of the crest is fully supported by a fresh supply of air at atmospheric pressure.

If viscous and surface tension effects are taken to be negligible within the normal operating parameters of the weir,then determining the head-discharge equation over a tilting weir converges upon an understanding of how C_d behaves as a function of the dynamic parameters h/p and $\sin\theta$. As Rouse (1932) speculated, the reduction in $\sin\theta$ is likely to have the same effect as increasing the h/p ratio, by which the streamlines become more horizontal over the crest and the contraction coefficient increases to allow more discharge over the weir, given the same upstream head condition. The goal of this study is to determine the nature of the relationship of C_d to h/p and $\sin\theta$ for tilting weirs, as well as the range of Reynolds number (Re) and Weber number (We) values that can be considered as a normal operating regime for free flow.

REVIEW OF PREVIOUS WORK

Sharp-Crested Weirs

Much careful experimental work was completed on the flow measurement equation for sharp-crested weirs from the late-nineteenth until the mid-twentieth century to find an empirical equation to relate C_d (as in Eq. 4) to h/p under normal operating conditions, *i.e.* when Re and We effects can be neglected. Notable works on this topic are those of Smith (1886), Bazin (1888), Rafter (1900), Horton (1906), Schoder and Turner (1929), Rehbock (1929), and USBR (1938).

The seminal work on the topic that aimed to integrate the work of previous researchers, while offering a large amount of new experimental data, was that of Kindsvater and Carter (1957). These researchers at Georgia Tech University offered the novel contribution of taking into consideration viscous and surface tension effects that become relevant at low values of h. They also considered the effect on the flow dynamics for weirs where $b/B < 1$. Kindsvater and Carter (1957) convincingly showed that earlier formulas for C_d in Eq. (4) of a nonlinear form were overly complex, and that a simple linear equation could be used instead. They also suggested the use of empirically calibrated correction factors, k_h and k_b to account for Re and We scale effects under small values of h and b, introducing equivalent head (h_e) and equivalent crest length (b_e) terms to obtain an effective

discharge coefficient (C_e) for sharp-crested weirs:

$$C_e = \frac{Q}{\frac{2}{3}\sqrt{2g}\, b_e h_e^{3/2}} \approx 0.602 + 0.075 h/p \tag{8}$$

with

$$h_e = h + k_h \tag{9}$$

$$b_e = b + k_b \tag{10}$$

The authors recommended the use of a k_h value of 0.003 ft, or approximately 1 mm. The use of of k_h is important only when values of h are small. For water flow through air, Kindsvater and Carter (1957) estimated that prediction error due to viscous and surface tension effects would be within 2% as long as $h > 0.06$ m. It was also emphasized that k_h is an empirically calibrated correction factor that could differ significantly depending on which set of experimental data was used. The original authors attributed this to differences in experimental equipment. However, we hypothesize that this discrepancy may be due to the fact that at low values of h, either We or Re effects can be dominant depending on whether the nappe is fully formed or not. Evidence for this bifurcation in the flow behavior at low h is given in Zhang et al. (2010). By giving k_h as a positive parameter, Kindsvater and Carter (1957) implicitly assumed We effects to be dominant at low values of h, as explained earlier. Therefore, the specific choice of k_h may be a point in need of finer calibration on a case by case basis, but we report here the recommended value $k_h = 0.001$ m of the original authors. A less uncertain choice is the value of k_b, which Kindsvater and Carter (1957) allowed to vary depending on the contraction ratio of the weir. They recommended a k_b value of -0.003 ft (-1 mm) for the case where $b/B = 1$.

After the work of Kindsvater and Carter (1957), several other publications have further elucidated the nature of sharp-crested weir flow over a wide range of h/p values, including measurements of velocity and pressure distributions near the crest. (Rajaratnam and Muralidhar 1971; Ramamurthy et al. 1987; Swamee 1988; Sinclair et al. 2022).

Tilting Weirs

With the early explorations of the sharp-crested weir as a flow measurement device, examinations were also made to investigate the effect that tilting the upstream face of the weir had on the nappe profiles and the head over the crest at a constant discharge (Bazin 1888; USBR 1938; Abou Seida and Quaraishi 1976). Hager (1994) compiled the data of several of these types of studies to develop a flow-rating equation for tilting weirs of the form:

$$Q = \left[\frac{2}{3}C_e + 0.05 \sin\left(\frac{3}{2}(90 - \theta)\right)\right] b\sqrt{2g}h^{3/2} \tag{11}$$

where C_e is Eq. 8 of Kindsvater and Carter (1957), the effective discharge coefficient for a sharp-crested weir. The second term in the brackets on the RHS of Eq. 11 accounts for the effect of the changing θ on the overall discharge capacity of the structure. This study, published in German, represents an interesting first investigation into the flow-rating equation of a tilting weir. However, it was limited by the fact that the early exploratory studies cited by Hager (1994) and used for calibration did not cover a wide range of flow conditions (i.e. h/p values).

The seminal work to date attempting to develop a flow-rating equation for tilting weirs is that of Wahlin and Replogle (1994). The authors of this technical report studied two models in a large flume (B = 1.2 m). As predicted earlier by Rouse (1932), they began with the assumption that the general form of the sharp-crested weir rating equation as given by Kindsvater and Carter (1957) in Eq. (8), could be applied to the modified case of the tilting weir with the addition of a corrective factor to account for variation in θ. They chose to call this term C_a. By studying data previously collected by the US Bureau of Reclamation (USBR) in analysis of the nappe profiles for flow over variously inclined weirs (USBR 1938), the authors hypothesized that the relation between C_a and θ would take the form of a second order concave polynomial. C_a can also be thought of as a discharge amplification factor, Q_θ/Q_{90}, which represents the relative effect of θ on the amount of discharge that is able to pass over the structure at a given head, compared to the perpendicular 90° case. The results of the study proved to be fairly true to the original hypothesis, and a second order

polynomial was defined as: $C_a = 1.0333 + 0.003848\theta - 0.000045\theta^2$, with θ in degrees. Although by definition C_a should be unity when $\theta = 90°$, the authors did not verify this experimentally, and their empirical equation for C_a does not reflect this.

Furthermore, the number of observations in their study for $\theta > 45°$ were limited. For $\theta = 54.2°$, 14 data points were collected over an h/p range of 0.11-0.3 ($0.04 < h < 0.11$ m), and for $\theta = 63.4°$ only seven observations were made over an h/p range of 0.09-0.22 ($0.03 < h < 0.09$ m). With such small values of h, the observations may have been subject to We and Re scale effects (Rehbock 1929; Kindsvater and Carter 1957). Thus, it is a concern of the current authors as to whether applying the inclination-angle correction factor given by Wahlin and Replogle (1994) for $\theta > 45°$ is advisable. Wahlin and Replogle (1994) did report that when using their approach for $20° < \theta < 45°$, an average percent error of only 0.8% was found in their predictions of the laboratory data. At the very least, this means there was low prediction bias for their approach within this range of θ. From the experimental data published in the appendix of the study, the current authors computed the mean absolute value percent error (MAPE) to be 2.5% for this same case, which gives a more complete understanding of the magnitude of residual error from this approach. When the laboratory-derived equation to a field-scale structure, it was found that their equation under-predicted the discharge in the field by an average of 6.34% (Wahlin and Replogle 1994). This raises the question of how directly applicable laboratory-calibrated discharge-rating equations are to field conditions.

Since the first study of Wahlin and Replogle (1994) little convergence has been observed in the published experimental data on flow over the tilting weir. Prakash et al. (2011) conducted a laboratory experiment of flow over inclined rectangular notched weirs, with $\theta = 30°$, 45°, 60°, 75°, and 90°. They found that the discharge capacity of the structure increases as θ decreases, and proposed an equation containing two fourth-order polynomials to account for this effect that was accurate to within 10%. However, the authors did not validate their findings with previous experimental data for flow over sharp-crested weirs, and their data have since found little agreement with results published by subsequent authors.

Work completed in South Korea has focused on studying the flow characteristics of free and

submerged flow over tilting weirs, as well as how sedimentation patterns are affected by the inclination angle of the weir (Lee et al. 2014; Lee 2016; Lee 2018). These works have suggested incorporating the upstream total hydraulic head (H) into the tilting weir rating equation in order to model the effect of θ on the flow. However, this suggestion does not offer the most practical means of implementation in the field, where measuring the kinetic energy head in the approach channel is difficult. Unfortunately, these works have also yet to be published in English; thus their applicability to the wider engineering community remains obscure.

Nikou et al. (2016) investigated tilting weirs in a laboratory setting with different side contractions for $\theta = 20°$, $40°$, $60°$, $80°$, and $90°$. However, these authors made their observations over only a small number of discharge scenarios, which resulted in calibration of the empirical coefficients to only $\pm$ 15 % in prediction accuracy. Additionally, in a discussion piece, Khalili Shayan et al. (2018) convincingly showed that the assumption of the original authors that critical flow occurs over the weir crest was inaccurate.

Bijankhan and Ferro (2018) attempted to develop a rating equation for the tilting weir that was meant to be independent of the dynamic head over the structure as measure d by h/p. This form is simpler in the sense that it depends on fewer dynamic parameters, but also less accurate because it neglects how C_d increases linearly with h/p (Kandaswamy and Rouse 1957). Furthermore, Bijankhan and Ferro (2018) did not explain how a fresh air supply was provided underneath the nappe to ensure the condition of atmospheric pressure. From the experimental photos posted by the authors, it appears the flow was not sufficiently aerated and thus subject to inundation effects, especially at low θ values where the relative difference between the crest elevation and tailwater depth is small. Furthermore, in a discussion piece on a follow-up study that Bijankhan and Ferro completed over submerged tilting weirs (Bijankhan and Ferro 2020), Hajimirzaie and González-Castro (2021) revealed a flaw in the dimensional analysis of the original authors that introduces a spurious correlation between the independent and dependent dimensionless parameters. This leads to the perceived conclusion that C_d, as in Eq. 4, is independent of h/p. Several experimental investigations have shown that this conlusion is incorrect. (Kandaswamy and Rouse 1957; Wahlin

and Replogle 1994; Sinclair et al. 2022).

Other researchers have studied the flow characteristics of tilting weirs using numerical modeling. Mahdavi and Shahkarami (2020) utilized smoothed particle hydrodynamics to provide helpful visualizations of the flow field both upstream and downstream of the weir crest. The authors also validated their simulations with good agreement to available data from physical experiments, at least when $\theta = 90°$. However, the authors did not study a sufficiently large number of flow scenarios to accurately calibrate a head-discharge equation dependent on θ. Khatamipour et al. (2022) studied Reynolds-averaged Navier-Stokes (RANS) simulations of flow over tilting weirs in Open FOAM using a two-dimensional k-ϵ turbulence model over 12 flow cases. The authors observed similar behavior to Wahlin and Replogle (1994) in the relationship between Q_θ/Q_{90} and θ, but at smaller magnitudes of Q_θ/Q_{90} than the original study. It was also apparent from the published qualitative flow images that the flow was submerged for $\theta < 90°$, and thus not viable for calibrating a free-flow rating equation.

Most recently, Zerihun (2022) presented a flow-rating equation for tilting weirs derived from a first-principles approach using the Boussinesq-type energy equation for depth-averaged flow. This allowed for the creation of a numerical code that accounted for the presence of non-hydrostatic effects in the sub-critical to super-critical transition region near the crest of the tilting weir. The results of the numerical simulations agreed well with the experimental nappe profiles of Bazin (1888) and USBR (1938). However, the flow-rating equation presented by Zerihun (2022) lacks practical applicability in that it includes terms for which the slope of the free surface and overflowing nappe must be known a priori.

To summarize, the consensus on how to properly treat the influence of θ on the flow characteristics of a tilting weir has so far been lacking in the literature. The initially proposed approach of Wahlin and Replogle (1994) has not been sufficiently validated for $\theta > 45°$, and the large majority of subsequent work has been lacking in experimental rigor. More recent work on determining the effect of the flow attack angle over other types of weirs has further highlighted that the influence of θ should not be neglected (Schmocker et al. 2011). Higher-order approaches, such as that presented

by Zerihun (2022), offer promise for further exploration of this problem numerically but must also be clearly linked to methods for practical implementation. In pursuit of that, we present here a thorough experimental effort at two unique geometric scales that entails a large number of careful observations across all relevant θ and h/p values for channel flow.

EXPERIMENTAL SETUP AND MEASURING DEVICES

Experiments were first conducted in a recirculating flume manufactured by Armfield and located in the Environmental Fluid Mechanics Laboratory (EFML) at Colorado State University (CSU), USA. The flume was 5 m in length and 0.3 m wide, with a smooth neoprene channel bed and glass side walls. The flume slope was set to be horizontal. Beyond the inlet condition provided by the flume manufacturers, it was found necessary to install a honeycomb-like matrix of porous material at the flume inlet to straighten and normalize the incoming flow. Furthermore, a series of small roughness elements were installed just downstream of the honeycomb matrix in order to trip the turbulent boundary layer and reproduce as close as possible a fully-developed open-channel velocity profile. The downstream channel boundary condition was a free-overfall.

Nine tilting weir models were constructed at $\theta = 25.7°, 29.1°, 36.4°, 45°, 50°, 53°, 64°, 71.2°,$ and 90° by machining two sheets of smooth acrylic plastic of 12.7 mm (0.5 in.) thickness and adhering them together using a waterproof adhesive. The length of the weir plate (L), as shown in Fig. 2, was consistent between all models at 150 mm. The crest of each model was precisely cut to be "knife-edged", with the angle between the downstream-sloping crest and the parallel sides of the acrylic plates being 45°. Due to air entrainment caused by the plunging nappe, circular tubes of PVC plastic were also installed along the glass side walls of the flume to provide access to fresh air supply, as in shown in Fig. 3. This ensured that the air pocket beneath the overflowing nappe was fully aerated to atmospheric pressure. The diameter of these tubes was sized to 19 mm (0.75 in.) according to specifications detailed in Bos (1976).

Measurements of h and steady Q were made over a full range of flow conditions for each model, ranging from clinging/laminar flow at the minimum, to fully inundated flow at the maximum. At least 20 observations were made within the free-flow regime, where dynamic similarity is achieved

and the inertia of the flow is great enough to be free from scale effects caused by viscosity and surface tension, while also avoiding the under-pressurization of the nappe caused by inundated flow (see Table 1). These free-flow observations were used to calibrate C_e as a function of h/p for each model. Observations of h were made at a distance of 0.8 m upstream of the model crest using a vernier-type point gauge to an accuracy of ± 0.3 mm (0.001 ft). Measurement of steady Q through the flume was made using an electromagnetic flowmeter located within the supply pipe to the channel with an accuracy of ± 0.3 L/s (0.01 cfs). Measurements of water temperature also were taken, at an accuracy of ± 0.1°C in order to precisely calculate temperature-dependent values for μ and σ.

To ensure the initial results of the EFML experiments were both reproducible and scalable, follow-up experiments were conducted in a similar recirculating flume located in the Hydraulic and Hydromorphology Laboratory (HHLab) of the RiverLy research unit operating in the centre of the Institut National de Recherche pour l'Agriculture, l'Alimentation, et l'Environnement (INRAE) located in Lyon-Villeurbanne, France. This flume was larger than the EFML flume, at 1 m wide and 18 m in length, with a smooth glass channel bottom and side walls (see Fig. 3). These experiments were conducted in the same manner as the earlier EFML experiments, with some minor variations. Here, four tilting weirs of the same design as the EFML models were examined at $\theta = 33°, 44°, 59°,$ and 90°, and L was reduced to 126 mm. The crest location of each model structure was kept consistent at 11 m downstream of the flume inlet, which was a sufficiently long entrance length to ensure a fully developed velocity profile. Measurements of h were made 0.8 m upstream of the crest location using a trio of ultrasonic depth sensors measuring at 50 Hz and spaced evenly in the transverse direction across the 1 m wide channel. Measurements of steady Q were made using an electromagnetic flow meter recording at 50 Hz. The resultant time-series of h and Q were then averaged over 60 s to yield mean values, and the measurements of h were further averaged across the three sensors. The standard deviation in the measurements of h and Q were approximately 1 mm and 0.3 L/s, respectively.

RESULTS

Verification with Previous Experimental Work

The present goal is to utilize the tilting weir as a special case of the sharp-crested weir ($\theta = 90°$). In the interest of best-practice we choose here to verify our experimental results for the vertical sharp-crested weir, labeled as experiments K and O in Table 1. In Fig. 4, it can be seen that there is excellent agreement between the dimensionless rating equation of Kindsvater and Carter (1957), given by Eq. (8), and the experimental data for the sharp-crested weir observed within the current study. For the combined 47 observations shown in Fig. 4, the MAPE between the observed C_e, and that predicted by Eq. (8) is only 0.55 %. Also plotted is the C_e equation given in Rehbock (1929). It corresponds to: $C_e = 0.602 + 0.082(h/p)$. Rehbock recommended the use of this equation with a k_h value of 1.25 mm as a very close alternative to his equation for the "non-effective" discharge coefficient (i.e. $C_d = 0.605 + 0.08h/p$). The Rehbock (1929) equation has the same intercept as Eq. (8), but the slope does not match the current experimental data as well as that of Kindsvater and Carter (1957). Because these experiments were completed in relatively narrow channels of width $b = 0.3$ and 1 m, we chose to use the recommended k_b value of 0.001 m from Kindsvater and Carter (1957) for a full-width ($b/B = 1$) weir in a narrow-width channel. However, we found it unnecessary to implement the introduction of k_h because for our experiments K and O, we did not observe the artificial increase in C_e attributable to the decrease in h that occurs when We effects are present under clinging flow conditions. Rather, Re effects appeared to be dominant for these experiments. Therefore, for all of the data presented in the current study, k_h is taken as 0 m. We aim to define a threshold h value below which viscous and surface tension effects are significant.

Determining the Effect of the Varying Inclination Angle

Fig. 5 plots the data collected at the EFML for this study across all θ values and flow conditions examined, representing Q ranging from 4.1-30.5 L/s. An attempt also was made to study the flow characteristics over a model where $\theta = 20°$, but sufficient free flow conditions could not be achieved. Furthermore, as shown in Table 1, the maximum value of h/p for most experiments was approximately unity before the flow became inundated. This was due to the bed elevation remaining constant downstream of the weir. This $h/p = 1$ limit for free flow was earlier predicted

by Rehbock (1929) for channels where there is no drop in bed elevation downstream of the crest. HHLab data are shown in Fig. 6, representing Q ranging from 10.7-84.1 L/s. In these plots, C_e is calculated exactly as in Eq. (8), with k_b = -0.001 m and k_h = 0 m. It can be seen that for the linear equation representing the dimensionless head-discharge rating equation, given by the form $C_e = c + m(h/p)$, both the intercept (c) and slope (m) of this line tend to increase as θ decreases. This can be understood by realizing that the tilting weir is an obstruction to the flow, and the amount of obstruction presented to the flow by the weir depends upon θ. Generally, the streamlines over the crest become more horizontal as θ decreases and as h/p increases. Due to this reduction in the contraction of the overflowing jet, less upstream potential energy, represented by h, is needed for the flow to pass over the obstacle presented by the weir for a given discharge.

To account for this effect, we propose a transformation to the h term in a manner similar to that used by Kindsvater and Carter (1957) and originally examined by Rehbock (1929). These authors suggested a linear transformation of the h term to account for the presence of viscous and surface tension effects at low values of h for flow over a sharp-crested weir. In a similar fashion, one can understand the effect of the changing θ for flow over a tilting weir as primarily affecting the h term. The magnitude of this h term, representing the amount of potential energy required to pass a certain flow over the weir crest, changes in response to shifting modes of approach kinetic energy dissipation and momentum transfer, as brought on by the changing θ.

Whereas Kindsvater and Carter (1957) used a simple linear transformation to account for viscous and surface tension effects for the static sharp-crested weir, an additional nonlinear transformation must be utilized for the case of the variably tilting weir due to the additional degree of freedom introduced by θ. Here, the flow dynamics are influenced both by the changing value of θ and the relative inertial condition as defined by h/p. In keeping with the method of calculation of C_e used by Kindsvater and Carter (1957), we choose to retain the notation of h_e as it is defined by Eq. (9). However, it should be noted that for this study, h and h_e were equivalent since k_h was kept as 0 m. The purpose of our additional proposed correction factor is to transform the h_e observed over a tilting weir to the h_e that would be observed under the same discharge if the weir were completely

perpendicular to the bed (i.e. $\theta = 90°$) using a term we call k_θ. When applied to the h_e term, the head-discharge rating equation for a tilting weir becomes:

$$Q = C_e \frac{2}{3} \sqrt{2g} b_e (k_\theta h_e)^{3/2} \tag{12}$$

where $C_e = 0.602 + 0.075 h/p$ from Eq. (8), and h_e and b_e are given by Eqn. (9) and Eq. (10), respectively. It should also be noted that the h/p term embedded in (12) within the C_e term has not been transformed by k_θ or k_h, but is in fact the directly measured ratio at any value of θ.

For determining k_θ, the most relevant length scale in this flow scenario is in the vertical because this indicates the degree to which the pressure at the crest will deviate from hydrostatic due to the vertical momentum of the flow as it navigates the weir (Castro-Orgaz and Hager 2017). So, one can reasonably expect that k_θ could be understood most parsimoniously as being a function of $\sin\theta$, as was previously identified in our dimensional analysis. Using the independently measured discharge, unique values of k_θ can be found for each observation as in Eq. 13.

$$k_\theta = \left[\frac{Q}{C_e \frac{2}{3} \sqrt{2g} b_e h_e^{3/2}} \right]^{2/3} \tag{13}$$

For each experiment shown in Table 1, the average value of k_θ calculated by Eq. 13 was found and is given in Table 2. Then, a trail and error best-fit regression analysis was performed to fit an empirical function to the calibrated k_θ values. Gaussian, sum of sine, and power function fits were examined. The greatest agreement with the observed k_θ values in Table 2 was found using a two-term power function, which is given by Eq. 14.

$$k_\theta \simeq -\alpha (\sin\theta)^\beta + (1 + \alpha) \tag{14}$$

where for the current experimental data $\alpha = 0.07$ and $\beta = 4.5$. Eq. (14) is valid for $\theta = 25° - 90°$, with RMSE = 0.0094 (see Fig. 8).

Eq. 14 is monotonic in the range of realistic θ values for tilting weirs. The implicit assumption

in this approach is that the effect of the inclination on the contraction coefficient of the nappe is continuous, and that there is no intermediate value of θ between 0-90° which represents either a local maxima or minima in the discharge capacity for the tilting weir. This is an assumption supported by the hypothesis of (Rouse 1932) that the effect of increasing θ on the contraction coefficient would be akin to a decrease in h/p. As can be seen from Eq. 8 and Fig. 4, the influence of h/p on the discharge capacity of the weir also is monotonic.

The inclusion of the exponent β on the $\sin\theta$ term indicates that the effect of θ on the contraction of the streamlines around the crest is nonlinear. This is likely due to the separation zone that is present at higher values of θ, but eventually disappears below some threshold value. From a cursory analysis of Fig. 8, a first approximation of this threshold value can be given as $\theta \approx 60°$. Zerihun (2022) also identified a similar threshold value of θ for the influence of the separation zone in the flow dynamics. From the construction of Eq. 14, it is evident that when $\theta = 90°$, k_θ will be unity in Eq. (14), and Eq. (12) reduces to the classical sharp-crested weir rating equation given by Kindsvater and Carter (1957). At a minimum value of $\theta = 20°$, a maximum k_θ value of approximately 1.07 is applied to the head term. Physically, this means that the same discharge is passing over the structure inclined at $\theta = 20°$ with an 6.5 % reduction in h compared to that discharge passing over a sharp-crested weir inclined at $\theta = 90°$.

Analyzing Uncertainty and Considering Operational Constraints

In addition to the 392 free-flow depth-discharge observations shown in Table 1, 48 additional observations across θ values were observed, but were excluded from the calibration of Eq. (14) since these observations were made outside the normal operating regime of the tilting weir. This concerned flow at low values of h that was subject to scale effects due to viscosity and surface tension. Flows outside the normal operating regime were identified either visually by the presence of a clinging nappe, or by regression analysis. If the inclusion of a certain data point at a low value of h noticeably reduced the regression coefficient of the linear C_e vs. h/p equation shown in Figs. 5 and 6, it was excluded. These additional observations are included in Figs. 9 and 10 to show the influence of scale effects on the accuracy of the rating equation to predict discharge.

Fig. 9 shows a plot of C_e versus h/p computed from Eq. (12) for the 440 observed sets of Q, h, h/p and θ, in comparison to Eq. (8). In Fig. 10, $\%_{error}$ is defined as the relative percent difference between the observed discharge during experimentation (Q_{obs}) and the predicted discharge (Q_{pred}) given by Eq. (12):

$$\%_{error} = \frac{Q_{obs} - Q_{pred}}{Q_{obs}} \times 100 \tag{15}$$

It can be observed from Fig. 9 that there is a general relationship between h/p and $\%_{error}$, with $h/p = 0.6$ being an approximate divergence point below which $\%_{error}$ beings to grow. This value was previously identified by a separate study as an indicator of the lower threshold for the normal operating regime of a sharp-crested weir (Sinclair et al. 2022). For all observations of the current study, when $h/p \leq 0.6$, the mean of $|\%_{error}|$ is 1.75%. When $h/p > 0.6$, this value is reduced to 1.15%.

To explore thresholds related to Re and We scale effects, we also define updated Re and We numbers, where the length scale has been corrected by k_θ:

$$Re_\theta = \frac{\sqrt{g}(k_\theta h)^{3/2}}{\nu} \tag{16}$$

$$We_\theta = \frac{\rho g (k_\theta h)^2}{\sigma} \tag{17}$$

Figure 10 and Table 3 reveal the relationship between Re_θ, We_θ, and the relative percent error ($\%_{error}$) between the predicted and observed discharge for the 440 observations within the current study. Two flow regimes were identified. The threshold values of Re_θ and We_θ were identified by determining when the MAPE for the lower regime grew beyond 2 %, and the prediction bias, represented by the mean value of $\%_{error}$, was a close to zero as possible for the upper regime. We choose ±2% as a somewhat arbitrary threshold, but this level of accuracy can generally be considered as excellent for flow measurements over hydraulic structures (Replogle 2002).

Regime I occurs when $Re_\theta \leq 3 \times 10^4$ & $We_\theta \leq 3 \times 10^2$ and represents flow that occurs below the absolute minimum required inertial state in the approach for the weir to be considered operating

in free flow. Below this threshold, scale effects cannot be justifiably neglected. Fig. 10 and Table 3 show that for the majority of points, this results in the observed discharge being smaller than what is predicted for this regime, indicating that Re_θ effects were more significant here than those due to We_θ. This can be most readily explained by understanding that as viscous effects become more significant at low values of Re_θ, the piezometric head (h) must grow larger to account for the decrease in the velocity head. Regime II occurs when $Re_\theta > 3 \times 10^4$ & $We_\theta > 3 \times 10^2$. Here, scale effects are minimized and the accuracy of the head-discharge equation is optimized. This represents the ideal operating regime for a tilting weir. Table 3 shows that for this regime, the average $\%_{error}$ is only -0.08 %, indicating the bias in the predicted discharge has been removed compared to Regime I.

These threshold values for Re_θ and We_θ can also be translated to more practical values of h, if we assume common values for physical constants and the fluid properties of room-temperature water (i.e. $g = 9.81\ m/s^2$; $\mu = 10^{-3}\ Ns/m^2$; $\rho = 1000\ kg/m^3$; $\sigma = 0.0728 N/m$). These approximated values are shown in Table 3. Unsurprisingly, we find a similar result as Kindsvater and Carter (1957) for the threshold value of $h \approx 0.05$ m as the point above which scale effects can be justifiably neglected. A similar finding was also reported in Hager (1994), but Ranga Raju and Asawa (1977) advocate for a much higher threshold for avoiding scale effects of $h > 0.11$ m. The frequency histograms shown in Fig. 10 also can be used to estimate the probability of a certain level of measurement accuracy within each regime (see Table 3).

DISCUSSION

We now turn to some qualifications for the findings of the current study. First, it can be observed from the residuals in Fig. 8 that the greatest uncertainty in the the value of k_θ occurs between $\theta = 45°$ and $65°$. We hypothesize that this is partially due to experimental error and uncertainty in the aeration condition of the downstream nappe. Another possible explanation is the instability of the separation zone in this region. Additionally, in Fig. 8, it can be seen that a large gap in the observed k_θ values exists between the four experiments with $\theta > 60°$ and the remainder of the experiments. One possible explanation for this behavior could be the disappearance of the

separation zone below $\theta \approx 60°$, which merits further exploration.

An analysis of Fig. 7 reveals that k_θ may be dependent on h/p as well as $\sin\theta$. This dependence is observable for experiment D in Fig. 7; but a consistent dependence was not found between all experiments upon further investigation. Additional experimentation to investigate the link between k_θ with both h/p and $\sin\theta$ is warranted.

Finally, additional observations are needed for θ between 60° and 90°. The experimental data of the current study is sparse in this range, where the dynamics of the separation zone are likely to change most significantly. It also remains to be seen how applicable these laboratory findings can be when the flow problem is scaled up and implemented in the field. Additional complexities related to the amount of friction in the approach channel, the approach geometry, the impact of sedimentation over time, and changes to the surface roughness of the weir plate must be considered.

CONCLUSIONS

Observations of head and steady discharge were made for 440 flow cases in two unique experimental facilities, over hydraulic models of tilting weirs with inclination angles ranging from $\theta = 25°$ to 90°. This allowed for the calibration of a head multiplication term as a function of the inclination angle, given by k_θ in Eq. (14). This empirical equation accounts for the fact that at a constant discharge, the head upstream of a tilting weir generally decreases with the inclination angle, due to the improved navigability of the streamlines over the crest and reduction in non-hydrostatic effects near the crest. The factor k_θ then acts to adjust the observed head over a tilting weir to that expected if the weir was perpendicular to the channel bed. Then, a modified form of the classical sharp-crested weir rating equation, given by Eq. (12), can be applied to predict steady discharge. If the inertial state of the approach flow is kept above a threshold value of at least $Re_\theta = 3 \times 10^4$ & $We_\theta = 3 \times 10^2$ ($h \approx 0.05$ m) and the nappe remains fully aerated, the inclined rectangular can be considered within an ideal operating regime where the mean absolute value of the error in the predicted discharge is only 1.3 % for the current experimental data (see Table 3). We also identify an h/p value of 0.6 as a more immediately applicable threshold for the normal operating regime, but note that this value will likely not hold for especially small weirs (i.e. $L < 0.1$ m).

The results of this study work to synthesize and expand significantly upon the current level of knowledge within the literature. The most extensive study to date on developing a head-discharge rating equation for tilting weirs is that of Wahlin and Replogle (1994). The current study expands on this work by developing an equation having greater continuity with previous work, in that it links back to the classical empirical data for the sharp-crested weir, being applicable for $25° \leq \theta \leq 90°$. We also offer a more parsimonious monotonic solution to correct for the effect of the dynamic weir inclination angle that relies less on arbitrarily maximizing goodness-of-fit metrics for the observed empirical data, and instead aims to give insight to the underlying flow dynamics. In terms of calibration accuracy, the current study contains a much larger number of observations of the flow at θ between 45° and 90° than in previous studies. As shown by Fig. 11, this results in the data from the current study agreeing well with the findings of previous researchers for certain values of θ, while also being able to more fully reveal the nature of the relationship between Q_θ/Q_{90} and θ across a wide range of operational θ values. In summary, the findings of this study promote the tilting weir as a practical and versatile structure not only for stage regulation but also for flow measurement, giving operators of open-channel flows the opportunity for much greater control and efficiency over their system.

TOWARDS PRACTICAL IMPLEMENTATION

Step-by-step instructions taken from the approach laid out in this study for using the tilting weir as a water flow measurement structure are as follows:

1. Measure the inclination angle (θ) of the weir from the horizontal and the crest elevation (p) relative to the upstream channel bed.
2. Measure the depth of water flowing over the weir crest (h) at a distance of 3-4 times the anticipated h, upstream from the crest location. To ensure most accurate measurement, h should be greater than 0.05 m.
3. Calculate h/p.
4. Using h/p, calculate C_e from Eq. 8.

5. Calculate h_e and b_e using the recommended values of k_h and k_b of Kindsvater and Carter (1957), as shown by Eqs. 9 and 10, respectively.
6. Calculate k_θ using Eq. 14.
7. Using Eq. 12, estimate the discharge Q.

APPENDIX

DATA AVAILABILITY STATEMENT

Some or all data, models, or code generated or used during the study are available in a repository online in accordance with funder data retention policies at https://doi.org/10.5061/dryad.xksn02vn4.

ACKNOWLEDGEMENTS

This work was supported by the Colorado Agricultural Experiment Station under Grant No. COL00424, and the Republic of France under the Chateaubriand Fellowship in STEM. The authors thank the reviewers for their constructive comments and recommendations.

DISCLAIMERS

The authors declare that they have no known competing financial interests or personal relationships that could have appeared to influence the work reported in this paper.

NOTATION LIST

The following symbols are used in this paper:

p = elevation of the weir crest above the channel bed [L];

L = vertical height of weir when perpendicular [L];

h = piezometric head above the weir crest [L];

H = total hydraulic head above the weir crest [L];

θ = angle between the inclined weir and the horizontal channel bed;

b = length of weir crest [L];

Q = volumetric discharge [L^3/T];

q = unit discharge per weir crest length [L^2/T];

u = velocity of a jet issuing from a small orifice [L/T];

$\overline{U}$ = bulk (cross-section averaged) channel velocity [L/T];

α = kinetic energy correction factor;

g = gravitational acceleration constant [L/T^2];

ρ = fluid density [M/L^3];

μ = fluid dynamic viscosity [M/LT];

σ = fluid surface tension [M/T^2];

Fr = Froude number;

Re = Reynolds number;

Re_θ = θ-adjusted Reynolds number;

We = Weber number;

We_θ = θ-adjusted Weber number;

k_h = linear head correction term [L];

k_b = linear weir crest length correction term [L];

h_e = effective head as corrected by k_h [L];

b_e = effective crest length as corrected by k_b [L];

k_θ = nonlinear head multiplication factor;

continued from previous page:

m = linear slope;

c = linear intercept;

C_d = discharge coefficient;

C_e = effective discharge coefficient;

Q_θ/Q_{90} = flow amplification factor

SUPPLEMENTAL MATERIALS

REFERENCES

Abou Seida, M. and Quaraishi, A. (1976). "A flow equation for submerged rectangular weirs.." *Proceedings of the Institution of Civil Engineers*, 61(4), 685–696 Publisher: ICE Publishing.

Bazin, H. E. (1888). "Expériences nouvelles sur l'écoulement en déversoir." *Annales des ponts et chaussées*.

Bijankhan, M. and Ferro, V. (2017). "Dimensional analysis and stage-discharge relationship for weirs: A review." *Journal of Agricultural Engineering*, 48(1), 1–11 Publisher: Page Press Publications.

Bijankhan, M. and Ferro, V. (2018). "Experimental Study and Numerical Simulation of Inclined Rectangular Weirs." *Journal of Irrigation and Drainage Engineering*, 144(7), 04018012 Publisher: American Society of Civil Engineers (ASCE).

Bijankhan, M. and Ferro, V. (2020). "Experimental Modeling of Submerged Pivot Weir." *Journal of Irrigation and Drainage Engineering*, 146(3), 04020001 Publisher: American Society of Civil Engineers.

Bos, M. G. (1976). *Discharge Measurement Structures*. International Institute for Land Reclamation and Improvement, Wageningen, The Netherlands.

Castro-Orgaz, O. and Hager, W. H. (2017). *Non-hydrostatic free surface flows*. Advances in geophysical and environmental mechanics and mathematics. Springer, Cham, Switzerland.

Clemmens, A., Wahl, T., Bos, M., and Replogle, J. (2001). *Water measurement with flumes*

and weirs. International Institute for Land Reclamation and Improvement, Wageningen, The Netherlands ISBN: 907075455X.

Floodlist News (2017). "UK City of Leeds Installs Innovative Moveable Weirs FloodList." *Floodlist*, <https://floodlist.com/protection/leeds-flood-alleviation-moveable-weirs> (April).

Hager, W. H. (1994). "Dammüberfälle." *Wasser und Boden*, 46(2), 33–36 Place: Heidelberg Publisher: Springer.

Hajimirzaie, S. M. and González-Castro, J. A. (2021). "Discussion of Experimental Modeling of Submerged Pivot Weir by M. Bijankhan and V. Ferro." *Journal of Irrigation and Drainage Engineering*, 147(1), 07020012 Publisher: American Society of Civil Engineers.

Horton, R. E. (1906). *Weir experiments, coefficients, and formulas*, Vol. 16. US Government Printing Office.

Johnson, M. C. (1996). "Discharge coefficient scale effects analysis for weirs." Ph.D thesis, Utah State University, Logan, Utah. ISBN: 9780591027167.

Kandaswamy, P. K. and Rouse, H. (1957). "Characteristics of Flow over Terminal Weirs and Sills." *Journal of the Hydraulics Division*, 83(4), 1345–13 Publisher: American Society of Civil Engineers.

Khalili Shayan, H., Aminpour, Y., Peysokhan, P., and Bayrami, M. (2018). "Discussion of Extraction of the Flow Rate Equation under Free and Submerged Flow Conditions in Pivot Weirs with Different Side Contractions by N. Sheikh Rezazadeh Nikou, M. J. Monem, and K. Safavi." *Journal of Irrigation and Drainage Engineering*, 144(4), 07018008.

Khatamipour, B., Kavianpour, M. R., Khosrojerdi, A., and Ghodsi Hassanabad, M. (2022). "Numerical Study of Flow Characteristics Over Pivot Weirs." *Journal of Hydraulic Structures*, 8(3), 17–32 Publisher: Shahid Chamran University of Ahvaz.

Kindsvater, C. E. and Carter, R. W. (1957). "Discharge Characteristics of Rectangular Thin-Plate Weirs." *Journal of the Hydraulics Division*, 83(6), 1453–36 Publisher: American Society of Civil Engineers.

Lee, K. S. (2016). "Analysis of submerged flow characteristics of the improved-pneumatic-movable

weir through the laboratory experiments." *Journal of Korea Water Resources Association*, 49(7), 615–623 Publisher: Korea Water Resoureces Association.

Lee, K. S. (2018). "Experimental analysis of the sedimentation processes by variation of standing angle in the improved-pneumatic-movable weir." *Journal of Korea Water Resources Association*, 51(9), 795–802 Publisher: Korea Water Resoureces Association.

Lee, K.-S., Jang, C.-L., Lee, N., and Ahn, S. (2014). "Analysis of Flow Characteristics of the Improved-Pneumatic-Movable Weir through the Laboratory Experiments." *Journal of Korea Water Resources Association*, 47, 1007–1015.

Mahdavi, A. and Shahkarami, N. (2020). "SPH Analysis of Free Surface Flow over Pivot Weirs." *KSCE Journal of Civil Engineering*, 24(4), 1183–1194 Publisher: Springer Verlag.

Martínez, J., Reca, J., Morillas, M. T., and López, J. G. (2005). "Design and Calibration of a Compound Sharp-Crested Weir." *Journal of Hydraulic Engineering*, 131(2), 112–116 Publisher: American Society of Civil Engineers.

Nikou, N. S. R., Monem, M. J., and Safavi, K. (2016). "Extraction of the Flow Rate Equation under Free and Submerged Flow Conditions in Pivot Weirs with Different Side Contractions." *Journal of Irrigation and Drainage Engineering*, 142(8), 04016025 Publisher: American Society of Civil Engineers (ASCE).

Prakash, M. N. S., Ananthayya, M. B., and Kovoor, G. M. (2011). "Inclined Rectangular Weir-Flow Modeling." *Earth Science India*, 4(2), 57–67.

Rafter, G. W. (1900). "On the Flow of Water Over Dams." *Transactions of the American Society of Civil Engineers*, 44(2), 220–314 Publisher: American Society of Civil Engineers.

Rajaratnam, N. and Muralidhar, D. (1971). "Pressure And Velocity Distribution For Sharp-Crested Weirs." *Journal of Hydraulic Research*, 9(2), 241–248.

Ramamurthy, A. S., Tim, U. S., and Rao, M. V. J. (1987). "Flow Over SharpCrested Plate Weirs." *Journal of Irrigation and Drainage Engineering*, 113(2), 163–172 Publisher: American Society of Civil Engineers.

Ranga Raju, K. G. and Asawa, G. L. (1977). "Viscosity and surface tension effects on weir flow."

Journal of the Hydraulics Division, 103(10), 1227–1231 Publisher: American Society of Civil Engineers.

Rehbock, T. (1929). "Discussion of Precise Weir Measurements." *Transactions of the American Society of Civil Engineers*, 93(1), 1143–1162 Publisher: American Society of Civil Engineers.

Replogle, J. A. (2002). "Some Observations on Irrigation Flow Measurements at the End of the Millennium." *Applied Engineering in Agriculture*, 18(1), 47– Publisher: American Society of Agricultural and Biological Engineers.

Rouse, H. (1932). "The distribution of hydraulic energy in weir flow with relation to spillway design." M.S. thesis, Massachusetts Institute of Technology, Cambridge, Massachusets.

Rouse, H. (1946a). "Effects of Viscosity on Fluid Motion." *Elementary Fluid Mechanics*, John Wiley and Sons Inc., New York, NY, 167–168.

Rouse, H. (1946b). *Elementary Mechanics of Fluids*. John Wiley and Sons Inc., New York, NY.

Rouse, H. and Ince, S. (1963). *History of hydraulics*. Dover Publications, New York.

Sarginson, E. J. (1972). "The influence of surface tension on weir flow." *Journal of Hydraulic Research*, 10(4), 431–446.

Schmocker, L., Halldórsdóttir, B. R., and Hager, W. H. (2011). "Effect of Weir Face Angles on Circular-Crested Weir Flow." *Journal of Hydraulic Engineering*, 137(6), 637–643 Publisher: American Society of Civil Engineers.

Schoder, E. W. and Turner, K. B. (1929). "Precise Weir Measurements." *Transactions of the American Society of Civil Engineers*, 93(1), 999–1110 Publisher: American Society of Civil Engineers.

Sinclair, J. M., Venayagamoorthy, S. K., and Gates, T. K. (2022). "Some Insights on Flow over Sharp-Crested Weirs Using Computational Fluid Dynamics: Implications for Enhanced Flow Measurement." *Journal of Irrigation and Drainage Engineering*, 148(6), 04022011 Publisher: American Society of Civil Engineers.

Smith, H. (1886). *Hydraulics, the flow of water through orifices over weirs, and through open conduits and pipes*. Wiley, New York.

694 Stringam, B. L. and Gill, T. (2012). “Simplified Overshot Gate Constructed and Maintained by
695 Irrigation Districts.” *Irrigation and Drainage*, 61(5), 666–672.
696 Swamee, P. K. (1988). “Generalized Rectangular Weir Equations.” *Journal of Hydraulic Engineer-*
697 *ing*, 114(8), 945–949 Publisher: American Society of Civil Engineers.
698 USBR (1938). “Boulder Canyon project : final reports. Bulletin 3: "Studies of Crests for Over-
699 fall Dams".” *Report No. 6: Hydraulic Investigations*, United States Bureau of Reclamation,
700 Department of the Interior, Denver, Colo.
701 Wahlin, B. T. and Replogle, J. A. (1994). “Flow Measurement Using An Overshot Gate.” *Report*
702 *No. 1*, United States Bureau of Reclamation.
703 Zerihun, Y. T. (2022). “Free-flow discharge characteristics of an overshot gate: A non-hydrostatic
704 numerical modeling approach.” *Acta hydrotechnica*, 35(63), 101–115.
705 Zhang, X., Yuan, L., Peng, R., and Chen, Z. (2010). “Hydraulic Relations for Clinging Flow of
706 Sharp-Crested Weir.” *Journal of Hydraulic Engineering*, 136(6), 385–390 Publisher: American
707 Society of Civil Engineers.

List of Tables

TABLE 1. Description of experimental data collected. The number in parentheses after the number of observations per experiment (n) indicates the number of points used to calibrate the free-flow head-discharge equation. The range of h/p, Re_θ, and We_θ given for each experiment constitute the cases that were considered as free flow and used to calibrate the stage-discharge equation.

	Location	$\theta(^\circ)$	p (mm)	n	h/p		Re_θ		We_θ	
					min.	max.	min.	max.	min.	max.
A	EFML	25.7	65.0	27 (22)	0.50	0.94	2.0E+04	5.2E+04	1.6E+02	5.7E+02
B		29.1	73.0	26 (21)	0.57	0.91	2.9E+04	5.9E+04	2.7E+02	6.7E+02
C		36.4	89.0	36 (29)	0.36	0.98	2.0E+04	8.8E+04	1.6E+02	1.1E+03
D		45.0	106	43 (39)	0.38	0.97	2.7E+04	1.1E+05	2.4E+02	1.6E+03
E		45.0	106	23 (22)	0.43	1.05	3.3E+04	1.3E+05	3.1E+02	1.9E+03
F		50.0	115	20 (20)	0.35	0.96	2.8E+04	1.2E+05	2.5E+02	1.8E+03
G		50.0	115	27 (27)	0.34	1.02	2.6E+04	1.3E+05	2.2E+02	2.0E+03
H		53.0	120	50 (43)	0.43	0.99	3.9E+04	1.4E+05	3.9E+02	2.1E+03
I		64.0	135	27 (27)	0.32	0.99	2.9E+04	1.6E+05	2.7E+02	2.6E+03
J		71.2	142	27 (24)	0.39	0.95	4.1E+04	1.6E+05	4.2E+02	2.5E+03
K		90.0	150	27 (26)	0.24	0.93	2.2E+04	1.6E+05	1.8E+02	2.6E+03
L	HHLab	33.0	68.6	32 (27)	0.53	1.08	2.4E+04	7.0E+04	2.1E+02	8.5E+02
M		44.0	87.5	25 (20)	0.53	0.99	3.4E+04	8.7E+04	3.3E+02	1.1E+03
N		59.0	108	28 (24)	0.41	0.88	3.0E+04	9.6E+04	2.8E+02	1.3E+03
O		90.0	126	22 (21)	0.38	0.96	3.2E+04	1.3E+05	3.0E+02	2.0E+03

TABLE 2. Mean and standard deviation values of k_θ distributions for each experiment.

Experiment	θ (°)	$\overline{k_\theta}$	σ
A	25.7	1.074	0.0081
B	29.1	1.064	0.0045
C	36.4	1.065	0.0083
D	45	1.050	0.0040
E	45	1.042	0.0040
F	50	1.064	0.0025
G	50	1.066	0.0036
H	53	1.053	0.0016
I	64	1.009	0.0047
J	71.2	1.012	0.0034
K	90	1.000	0.0022
L	33	1.055	0.0055
M	44	1.054	0.0070
N	59	1.043	0.0032
O	90	1.000	0.0038

TABLE 3. Relationship between head-discharge equation prediction accuracy and inertial regimes as defined by Re_θ and We_θ. For use as a best practice guide for the normal operating regimes of tilting weirs.

Regime	Re_θ	We_θ	$\approx h$ (cm)	n	prob. ±2%	$\overline{\%_{error}}$	$\overline{\lvert\%_{error}\rvert}$
I	$\leq 3 \times 10^4$	$\leq 3 \times 10^2$	$h \leq 5$	72	0.53	-1.45	2.08
II	$> 3 \times 10^4$	$> 3 \times 10^2$	$h > 5$	368	0.80	-0.08	1.25

List of Figures

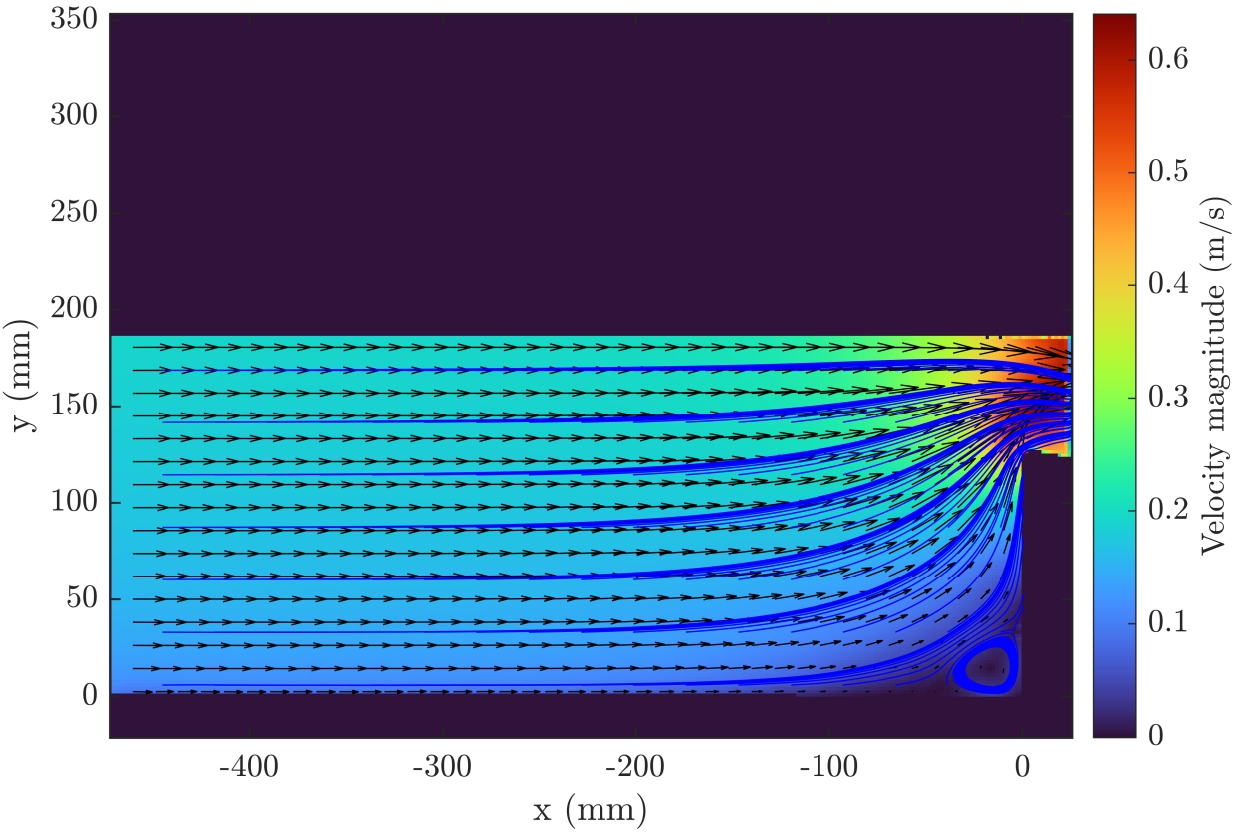

Fig. 1. Velocity magnitude vector field computed from particle-image velocimetry, with streamlines shown in blue. A zone of separated flow is apparent at the base of the weir. Flow case is from Experiment O at the HHLab; with $\theta = 90°$, $p = 126$ mm, and $Q = 30$ Lps.

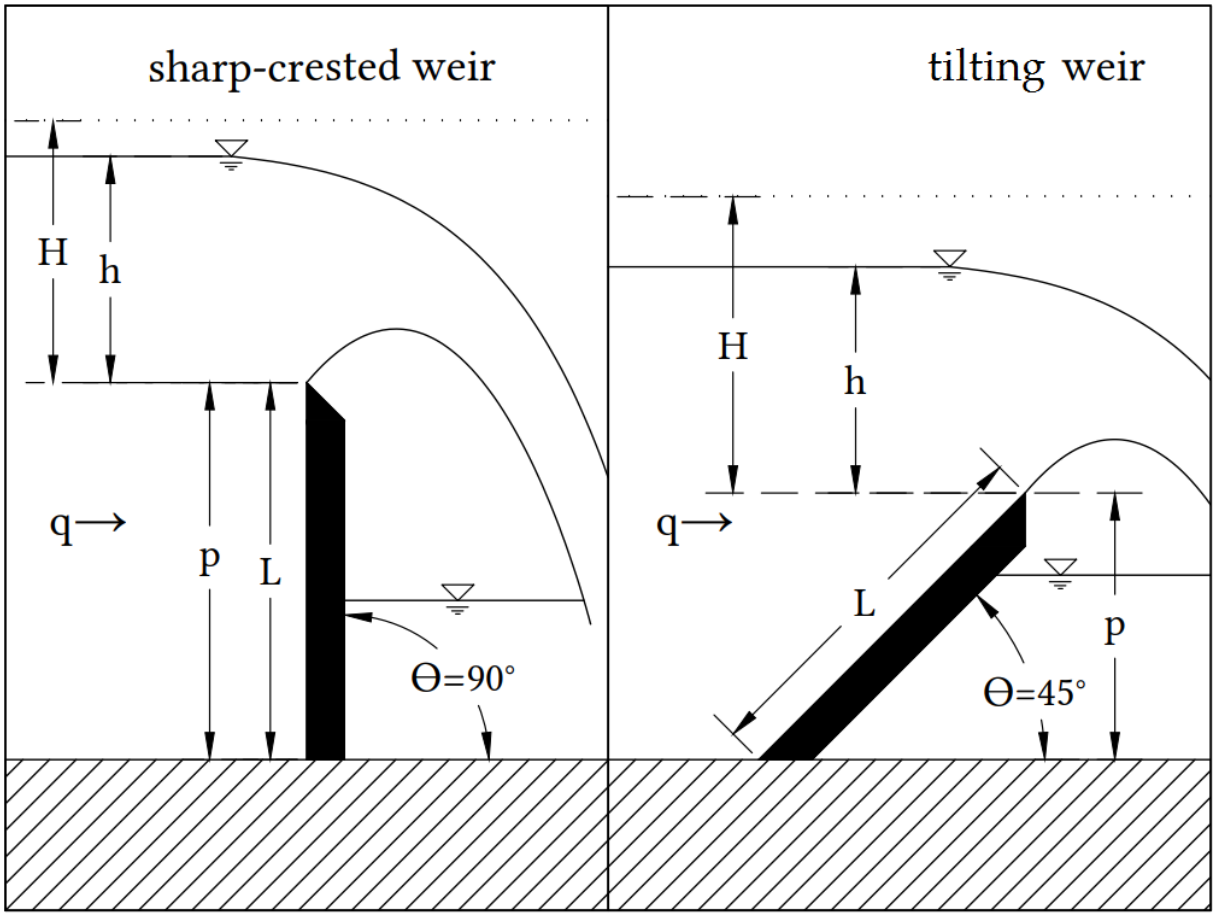

Fig. 2. Schematic of flow over a weir.

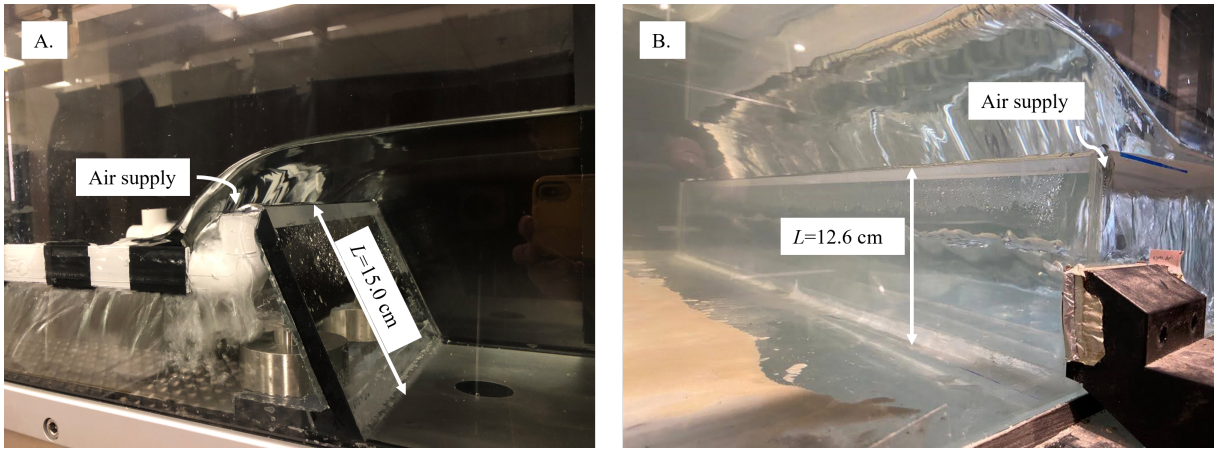

Fig. 3. Experimental setups in the Environmental Fluid Mechanics Laboratory (A.) and Hydraulic and Hydromorphology Laboratory (B), showing placement of aeration tubes downstream of the crest and the location where fresh air was supplied to the underside of the overflowing nappe.

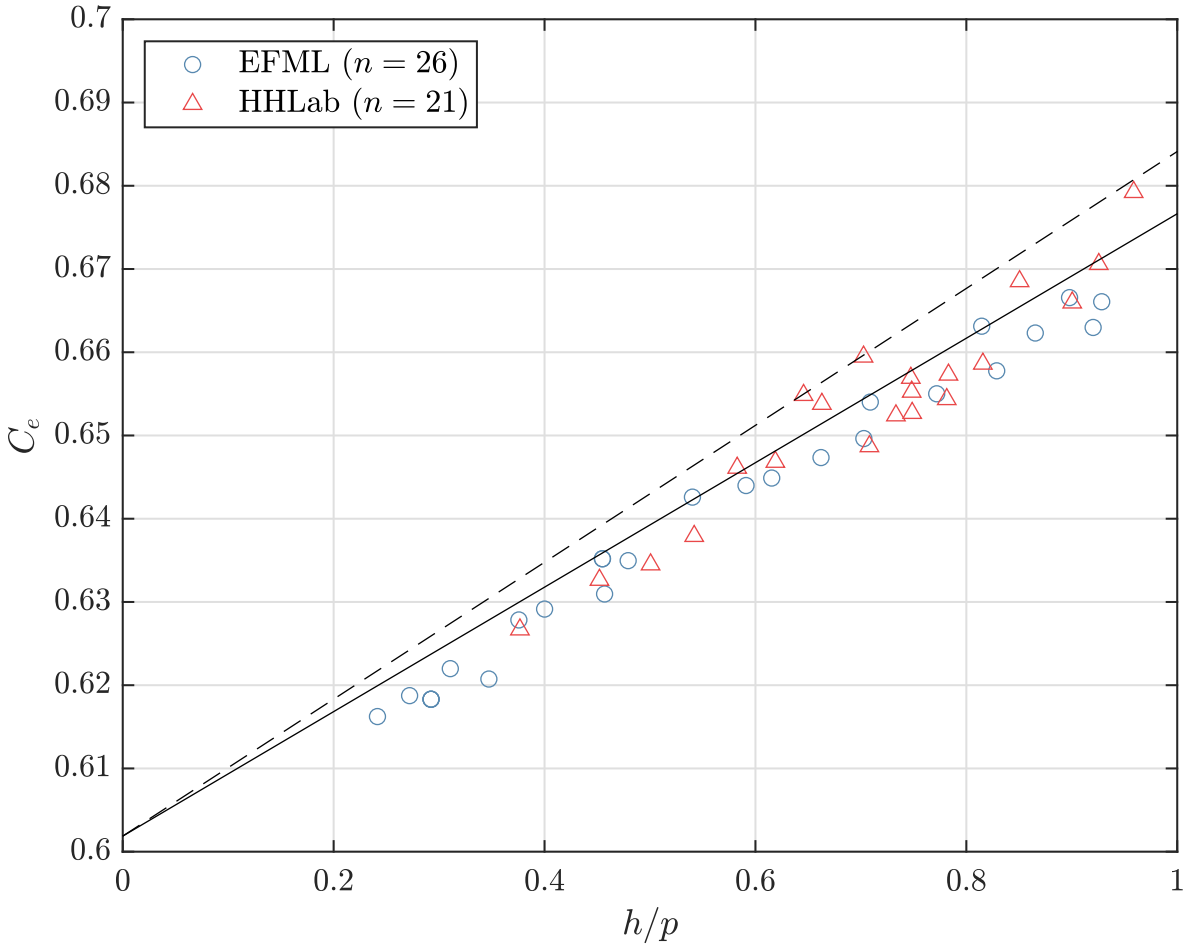

Fig. 4. Dimensionless stage-discharge plot comparing the results of the present study for a sharp-crested weir ($\theta = 90°$) with the best-fit equations of previous experimentalists. Data points are calculated as $C_e = Q/\frac{2}{3}\sqrt{2g}b_e h_e^{3/2}$, with $k_b = -0.001$ m and $k_h = 0$ m. The solid line corresponds to $C_e = 0.602 + 0.075h/p$ from Kindsvater and Carter (1957). The dashed line corresponds to $C_e = 0.602 + 0.082h/p$ from Rehbock (1929).

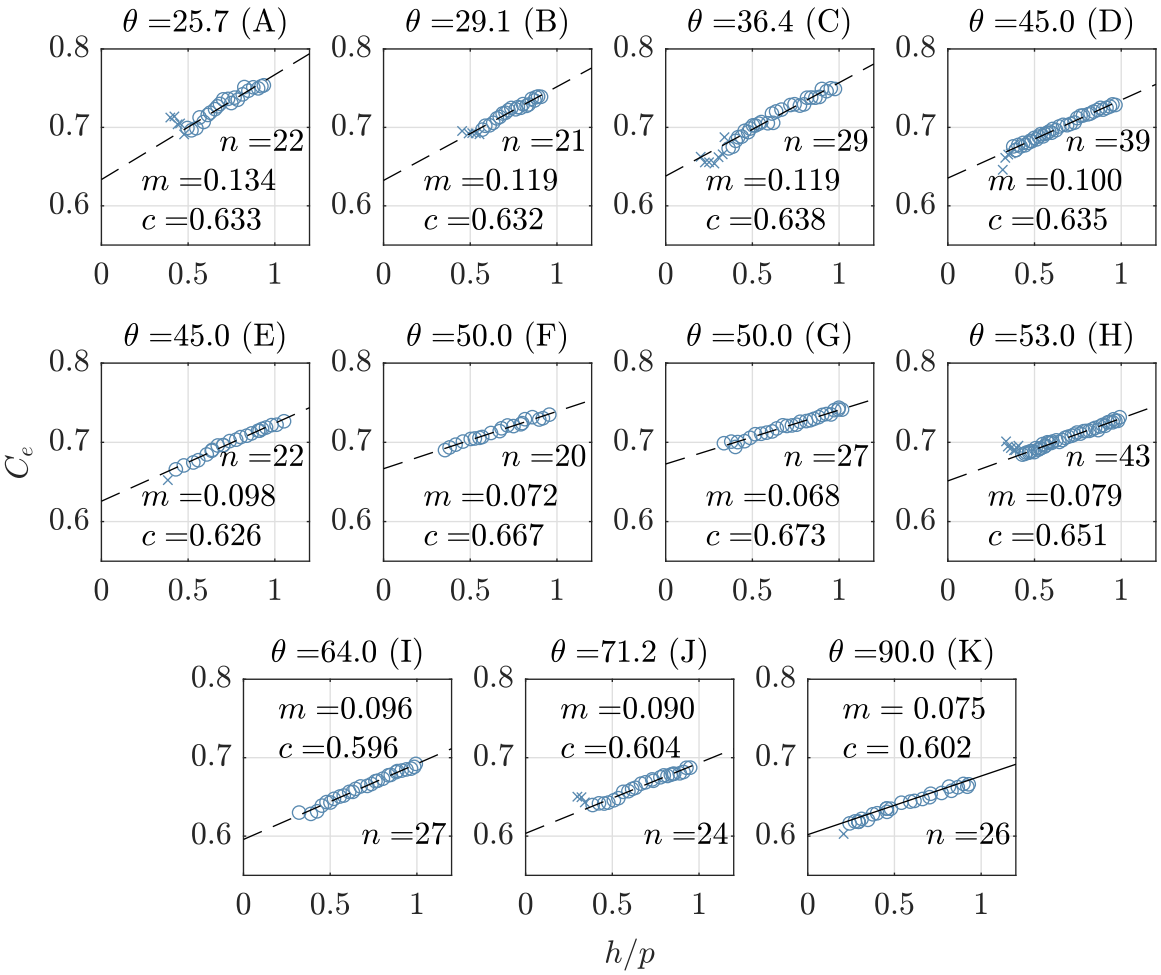

Fig. 5. Dimensionless plot of C_e versus h/p for each weir inclination angle studied for the EFML experiments, with the linear best fit equation obtained from least-squares regression shown in the form: $C_e = c + m(h/p)$. Here, $C_e = Q/\frac{2}{3}\sqrt{2g}b_e h_e^{3/2}$, with $k_b = -0.001$ m and $k_h = 0$ m. Data points considered as free flow and used to calibrate the linear best fit equation are shown by circles and tallied by n. Data points excluded due to scale effects shown by 'x's.

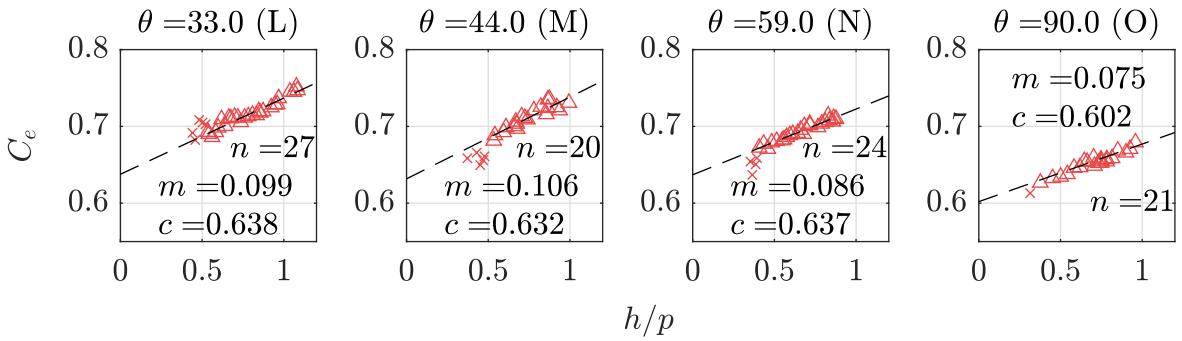

Fig. 6. Experimental data for tilting weir flow observed at the HHLab. See Fig. 5. Here data points considered as free flow and used to calibrate the linear best fit equation are shown by triangles.

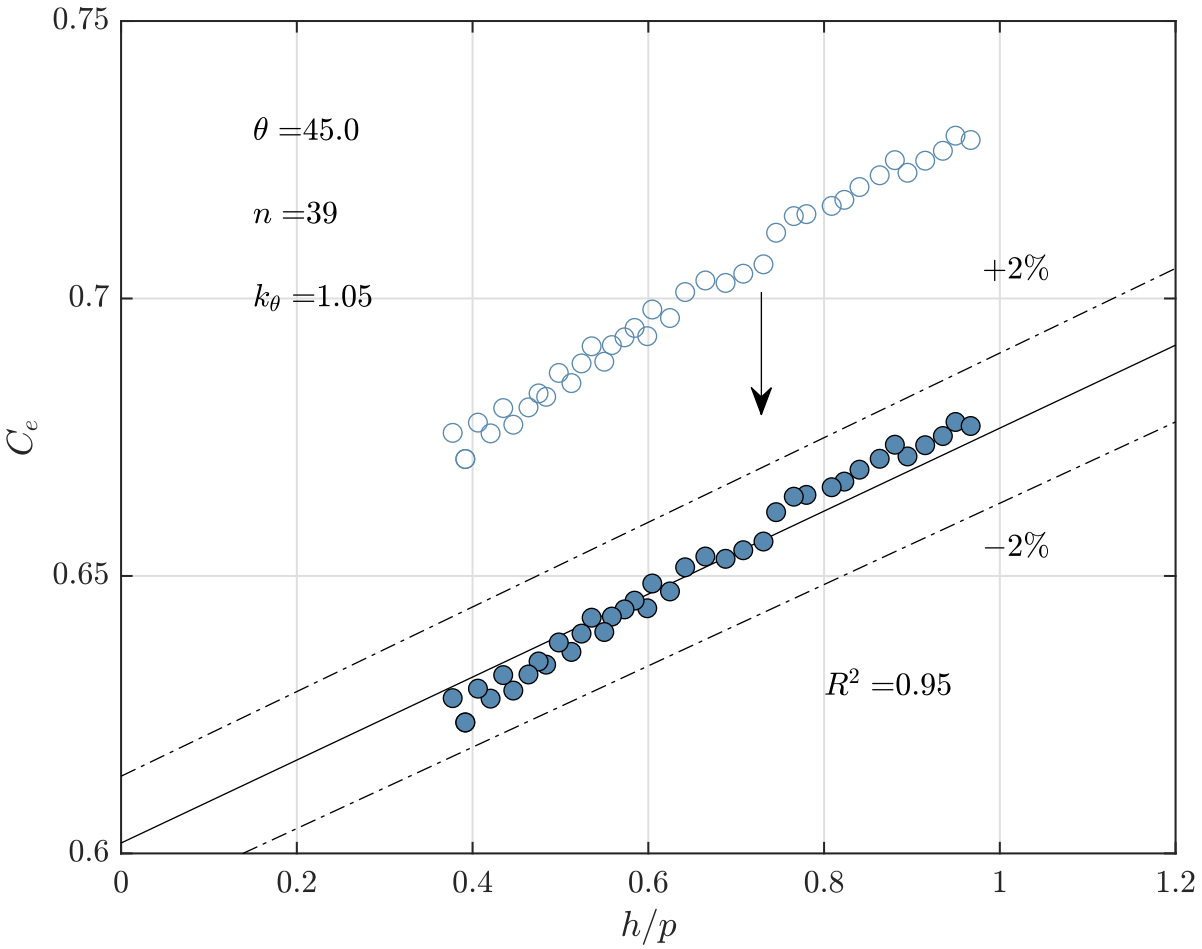

Fig. 7. Example transformation of C_e values for constant h/p by way of k_θ head multiplication factor, from Experiment D. For the original values, shown by the hollow circles, $C_e = Q/\frac{2}{3}\sqrt{2g}b_e h_e^{3/2}$, with $k_b = -0.001$ m and $k_h = 0$ m, as in Fig. 5. For the transformed values, shown by the filled circles, $C_e = Q/\frac{2}{3}\sqrt{2g}b_e(k_\theta h_e)^{3/2}$, with $k_\theta = 1.05$. Also shown is the R^2 value for the transformed values with respect to Eq. (8), given by the solid line, with ± 2% deviation shown by the dashed lines.

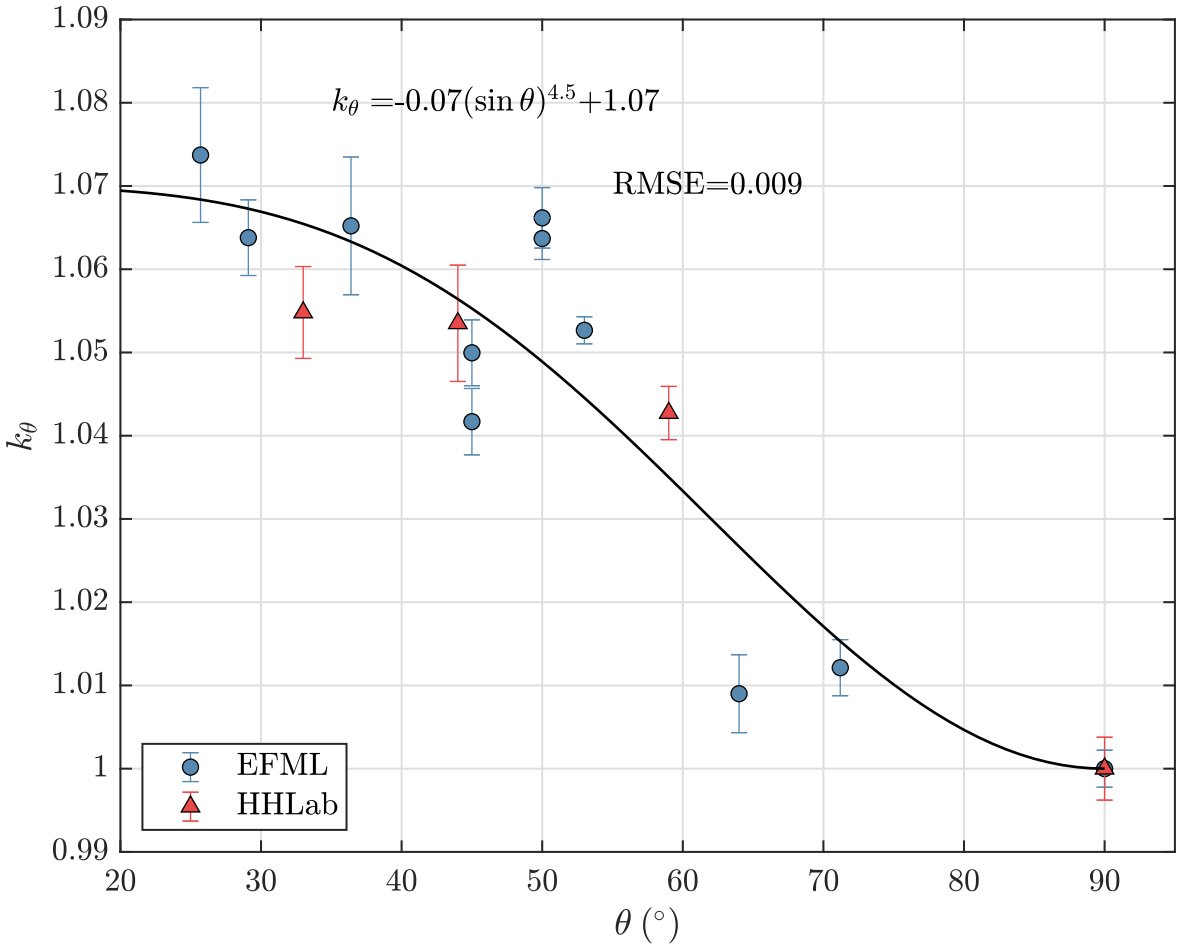

Fig. 8. Empirical data and best-fit curve for the relationship between θ in degrees with the head correction factor k_θ. Mean values of k_θ are shown for each experiment with error bars representing $\pm\sigma$, as in Table 2.

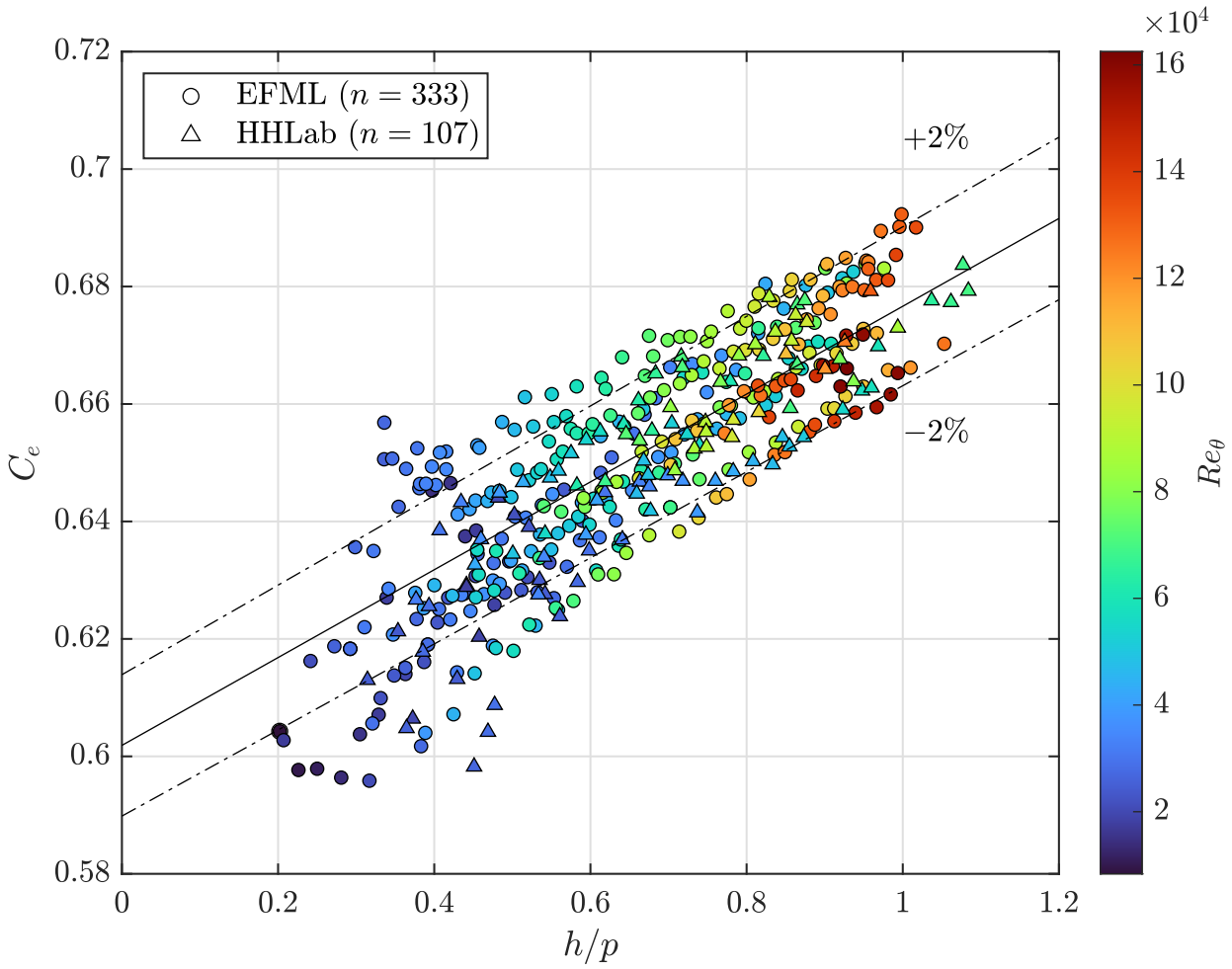

Fig. 9. Scatter plot of C_e versus h/p for total of 440 observations after tilting weir h values have been corrected by the k_θ values given by Eq. (14). The solid line with ± 2 % deviation is Eq. (8) and represents the predicted flow by Eq. (12). The Re_θ (defined by Eq. 16) colorbar is shown to indicate how the deviation from the predicted C_e to the observed grows as Re_θ decreases.

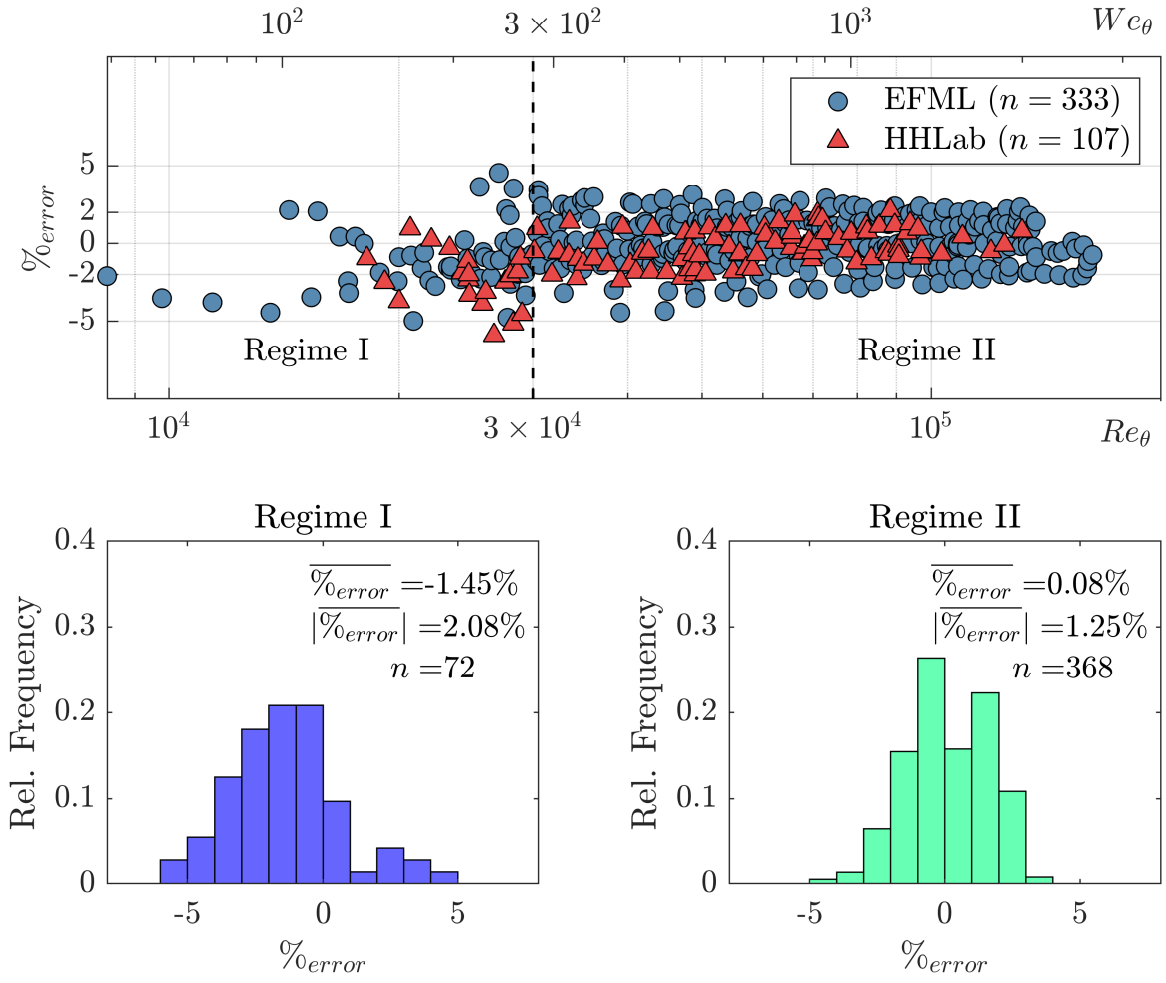

Fig. 10. Top: scatter plot of 440 flow observations showing the relationship between prediction accuracy and Re_θ & We_θ. Bottom: frequency histograms of distribution of $\%_{error}$ for the two flow regimes identified.

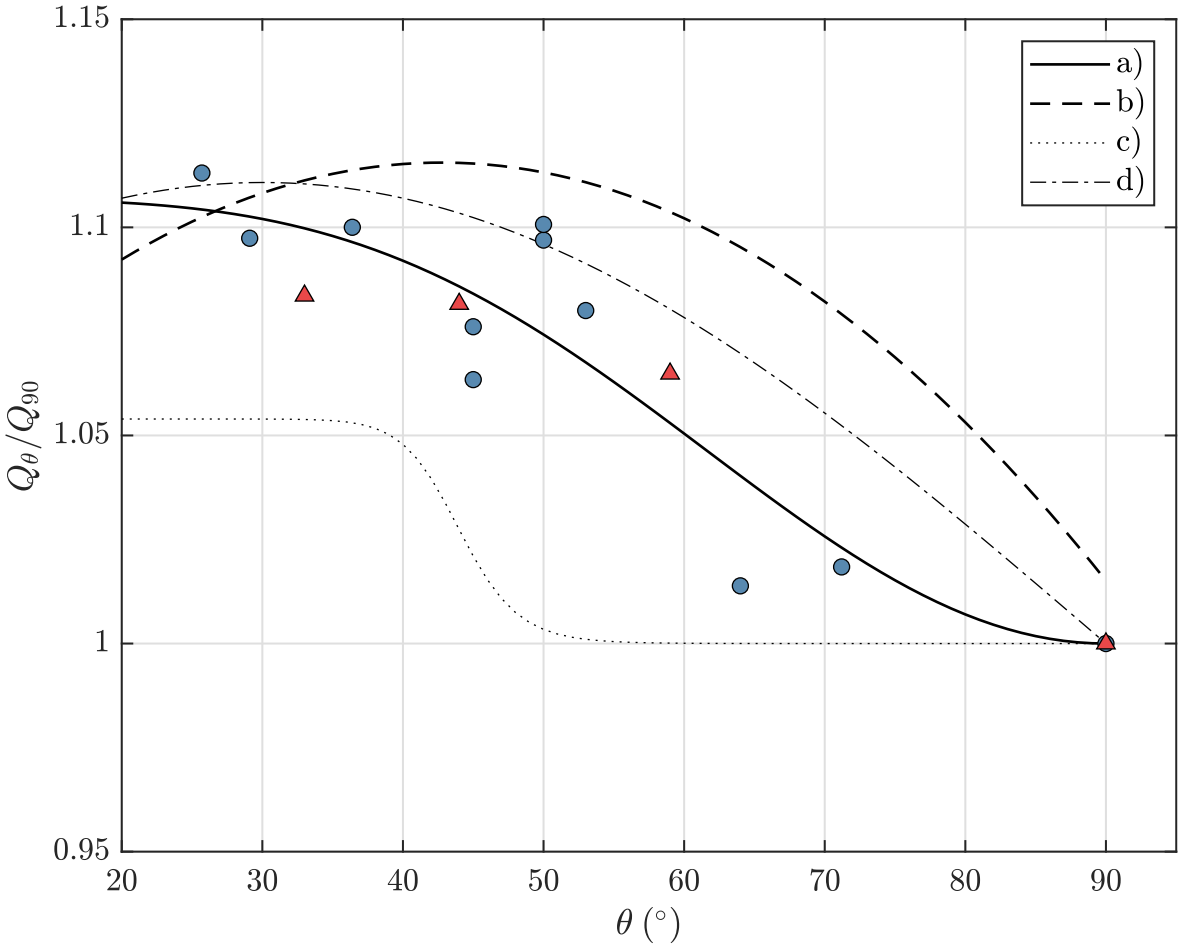

Fig. 11. Comparison of current and previous study results on the relative effect of the changing θ on Q for a given value of h. a) Eq. (14) of the current study, taken to the 3/2 power. Blue circles are EFML data, and red triangles are HHLab data. b) Wahlin and Replogle (1994). c) Bijankhan and Ferro (2018). d) Hager (1994).